ChemComm

Visible Light-Driven CO2 Reduction with a Ru Polypyridyl Complex Bearing an N-Heterocyclic Carbene Moiety

Journal:	*ChemComm*
Manuscript ID	CC-COM-02-2022-000657.R1
Article Type:	Communication

COMMUNICATION

Visible Light-Driven CO_2 Reduction with a Ru Polypyridyl Complex Bearing an *N*-Heterocyclic Carbene Moiety

Received 00th January 20xx,
Accepted 00th January 20xx

DOI: 10.1039/x0xx00000x

Taito Watanabe,[a] Yutaka Saga,*[ab] Kento Kosugi,[a] Hikaru Iwami,[a] Mio Kondo*[abc] and Shigeyuki Masaoka*[ab]

A novel Ru polypyridyl complex with an *N*-heterocyclic carbene ligand was successfully synthesised and characterised. The complex exhibited an intense absorption band in the visible-light region derived from the strong electron-donating character of the carbene ligand, and efficiently catalysed the visible light-driven CO_2 reduction with the reaction rate of 36.7 h^{-1}.

The visible-light-driven reduction of CO_2 is considered a promising solution for energy and environmental problems[1,2] because this technology enables the conversion of the greenhouse gas CO_2 into energy-rich compounds by utilising renewable energy sources such as sunlight. Thus, extensive efforts have been devoted to the construction of molecule-based catalytic systems for the visible-light-driven reduction of CO_2.[3,4] Conventional catalytic systems usually consist of two distinct functional units: a photosensitiser for harvesting light and a catalytic centre for chemical conversion. However, the construction and/or understanding of the reaction mechanism of such systems often require complicated processes.

We previously reported the catalytic activity of a mononuclear Ru complex bearing a phosphine ligand, $[Ru^{II}(tpy)(pqn)(MeCN)]^{2+}$ (**RuP**, tpy = 2,2′:6′,2″-terpyridine; pqn = 8-(diphenylphosphanyl)quinoline; MeCN = acetonitrile, Fig. 1 (a)), for visible-light-driven CO_2 reduction.[5] **RuP** is a function-integrated photocatalyst that serves as a photosensitiser as well as a catalyst for CO_2 reduction. Visible-light-driven CO_2 reduction could be achieved by simply using **RuP** as a photocatalyst (i.e. without the need for additional photosensitisers). This complex is the first example of a Ru-based function-integrated photocatalyst for visible-light-driven

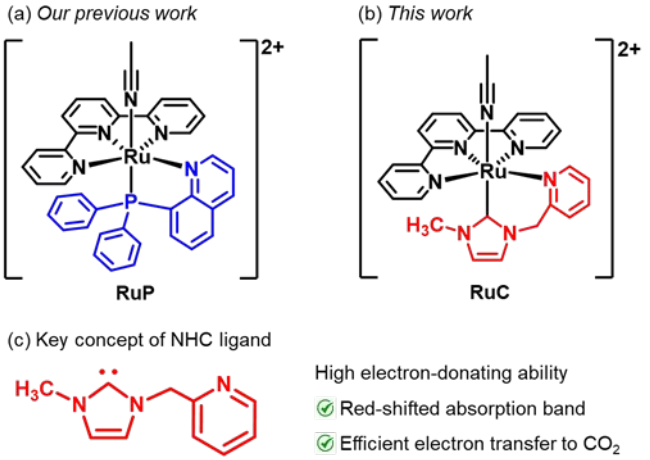

Fig. 1 Chemical structures of (a) **RuP** and (b) **RuC**, and the (c) key concept of an N-heterocyclic carbene (NHC) ligand.

CO_2 reduction, which offers a novel strategy for constructing catalytic systems for visible-light-driven CO_2 reduction. However, although the CO production rate of **RuP** is higher than those of other relevant function-integrated systems containing Re[6-11], Fe[12,13], Ir[14-20], Os[21,22], or Ru[5,23] as a metal centre, the construction of high-efficiency function-integrated catalysts remains a challenging endeavour.

Here, we demonstrate the development of a novel function-integrated Ru polypyridyl complex for efficient visible-light-driven CO_2 reduction. The precise modulation of the ligand structure resulted in the formation of a complex with a stronger visible-light absorption band and more electron-rich Ru centre compared with those of **RuP**. Such properties led to an over two-fold improvement in catalytic activity in terms of turnover frequency (TOF) compared with **RuP**. Indeed, the TOF of this new complex is higher than those of previously reported function-integrated catalysts for visible-light-driven CO_2 reduction.

The key to our success is the introduction of an *N*-heterocyclic carbene (NHC) ligand into the Ru polypyridyl complex (Fig. 1(b) and 1(c)). As demonstrated previously, **RuP**

[a] Department of Applied Chemistry, Graduate School of Engineering, Osaka University, 2-1 Yamadaoka, Suita Osaka 565-0871, Japan
[b] Innovative Catalysis Science Division, Institute for Open and Transdisciplinary Research Initiatives (ICS-OTRI), Osaka University, Suita, Osaka 565-0871, Japan
[c] PRESTO, Japan Science and Technology Agency (JST), 4-1-4 Honcho, Kawaguchi, Saitama 332-0012, Japan
* Corresponding authors. E-mail: ysaga@chem.eng.osaka-u.ac.jp, mio@chem.eng.osaka-u.ac.jp, masaoka@chem.eng.osaka-u.ac.jp
Electronic Supplementary Information (ESI) available: [details of any supplementary information available should be included here]. See DOI: 10.1039/x0xx00000x

can serve as a function-integrated catalyst. This fascinating property of **RuP** is achieved via the introduction of polypyridyl and phosphine ligands into its structure. The Ru polypyridyl scaffold affords a metal-to-ligand charge-transfer (MLCT)-derived absorption band in the visible-light region[24], and the *trans* influence of the phosphine ligand results in catalysis at a low overpotential.[25] In this study, we aimed to tune the absorption and catalytic properties of the complex by modifying the structure of its constituent ligands. NHC ligands have formal sp^2-hybridised lone pairs that can be donated to the σ-accepting orbitals of transition metals[26] and are widely used as excellent ligands for transition-metal for important catalytic chemical reactions. [27,28] Although the strong σ-donor and relatively weak π-acceptor properties of NHC ligands are similar to those of phosphine ligands, the former are generally known to have stronger electron-donating ability than the latter.[26,29] We thus believe that an NHC ligand can increase the electron density of the Ru centre. Therefore, we expect that the introduction of an NHC ligand into the Ru polypyridyl complex will enhance both the absorption and catalytic properties of the resultant complex, leading to the construction of a function-integrated catalyst with improved efficiency.

To this end, we designed a novel Ru complex, $[Ru^{II}(tpy)(cpic)(MeCN)]^{2+}$ (**RuC**, cpic = 1-methyl-3-(2'-picolinyl)-2*H*-imidazol-2-ylidene, Fig. 1(b)), with an NHC ligand. The synthesized **RuC** was identified by ^1H and ^{13}C NMR spectroscopy, ESI-MS, and elemental and single-crystal X-ray structural analyses (for details of the synthesis and characterisation procedures, see the Electronic Supplementary Information (ESI), P.S6-S16). The molecular structure of **RuC** was determined by single-crystal X-ray structural analysis, and the results are shown in Fig. S7. A summary of the crystallographic data is also presented in Table S1. Two chelate ligands, namely, tpy and cpic, coordinate with the metal ion in a perpendicular manner to form a distorted octahedral geometry at the Ru atom; here, the coordinated C atom of cpic and the MeCN ligand are in *trans* positions in the octahedron. Hereafter, **RuC** with tetraphenylborate (BPh_4) anion (**RuC**$(BPh_4)_2$) and **RuP** with hexafluorophosphate (PF_6) anion (**RuP**$(PF_6)_2$) were used for each measurement, unless otherwise mentioned.

Next, we investigated the photoabsorption properties of **RuC**. The UV-vis absorption spectrum of the complex (Fig. 2) exhibited an intense absorption band in the visible-light region centred at approximately 471 nm. The electronic transition of **RuC** was investigated using the time-dependent density functional theory (DFT) method. The calculated excitation wavelengths and oscillator strengths for selected transitions are listed in Table S6, and the absorption spectra based on these calculated transitions with Gaussian functions are depicted in Figure S17. The profiles of the convoluted absorption spectra were similar to those observed experimentally. The transitions in the visible-light region mainly arise from the MLCT transition from the dπ orbitals of Ru (HOMOs, Figure S13) to the π* orbitals of tpy (LUMO and LUMO+1, Figure S13). The MLCT band of **RuP** is centred at approximately 435 nm[5]. This result clearly demonstrates that the MLCT band of **RuC** is red-shifted compared with that of **RuP** and suggests that the strong

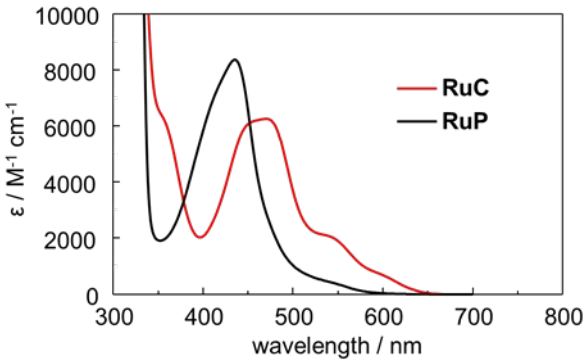

Fig. 2 UV-vis absorption spectra of **RuC** (red line) and **RuP** (black line) in MeCN (50 μM).

electron-donating ability of the NHC ligand increases the electron density of the central Ru ion.

Cyclic voltammetry (CV) was conducted under an Ar atmosphere to examine the electronic structure of **RuC** further. For the electrochemical measurement in the positive potential region, **RuC** with perchlorate (ClO_4) anion (**RuC**$(ClO_4)_2$) was used because BPh_4 anion exhibits redox wave in this potential region (Fig. S10). The CV profiles of **RuC** displayed a reversible one-electron oxidation wave, the half-wave potential ($E_{1/2}$) of which was +0.59 V *vs*. ferrocene/ferrocenium (Fc/Fc^+, Fig. 3(a), red line). The reversible oxidation wave at +0.59 V was assigned to the redox couple of Ru(III)/Ru(II)[24]. The oxidation potential of the Ru centre of **RuP** was observed at $E_{1/2}$ = +0.94 V (Fig. 3(a), black line), which is significantly higher than that of **RuC**. This result indicates that the electron density of the Ru centre is increased in **RuC** because of the stronger electron-donating nature of the NHC ligand compared with the phosphine ligand of **RuP**. In the negative-potential region, **RuC** exhibited two reversible one-electron reduction waves at $E_{1/2}$ = –1.72 and –2.03 V (Fig. 3(b), red line). DFT calculations (Figs. S13–S15) indicated that the first reduction wave at $E_{1/2}$ = –1.72 V could be attributed to the redox couple of tpy/tpy^- while the second wave at $E_{1/2}$ = –2.03 V could be assigned to the redox couple of tpy^-/tpy^{2-}. Under identical conditions, tpy in **RuP** is reduced at –1.73 V[24], which indicates that the energy levels of the LUMOs of **RuC** and **RuP** are nearly identical. The results of the electrochemical measurements collectively indicate that the energy level of the HOMO of **RuC** is sufficiently increased compared with that of **RuP**, whereas the energy levels of their LUMOs remain unchanged. This observation is consistent with the results of UV-vis absorption spectroscopy, which indicates that the MLCT band of **RuC** is significantly red-shifted compared with that of **RuP**.

RuC was subjected to CV experiments under CO_2 to examine the reactivity of the complex with CO_2. As shown in Fig. 3(c), current enhancement was observed at approximately –1.72 V in the presence of CO_2. The addition of H_2O to 2.65 M concentration in MeCN as a weak Brønsted acid to the test solution resulted in further current enhancement (Fig. 3(c), purple line). These results suggest an interaction between the one-electron reduced state of **RuC**, $[Ru^{II}(tpy^-)(cpic)(MeCN)]^+$ (**RuC**$^-$), and CO_2. This interaction is also observed for **RuP**, which

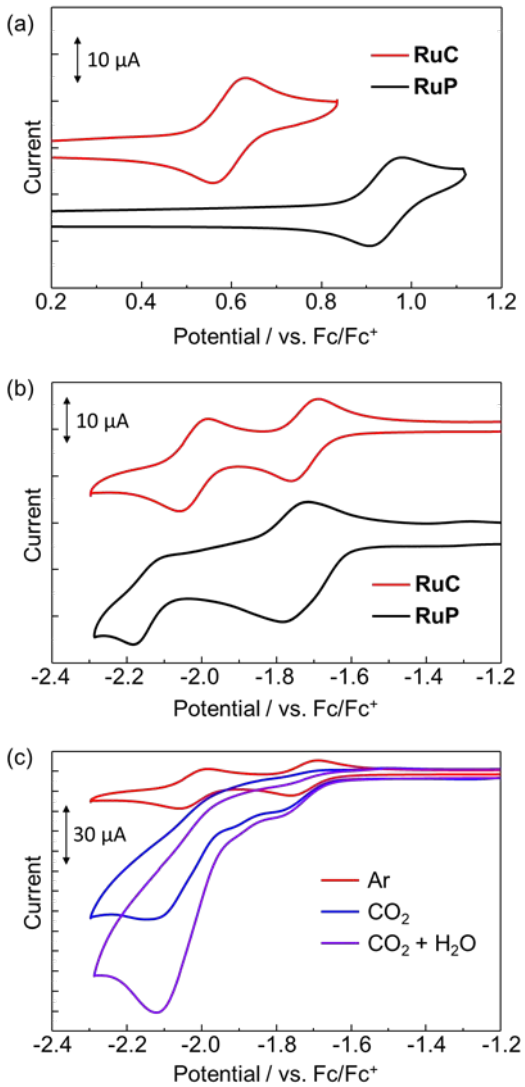

Fig. 3 Cyclic voltammograms (CVs) of **RuC** (0.5 mM) in 0.1 M tetrabutylammonium perchlorate/MeCN and **RuP** (0.5 mM) in 0.1 M tetraethylammonium perchlorate/MeCN under Ar (a) in positive potential region and (b) in negative potential region. (c) CVs of **RuC** in 0.1 M TBAP/MeCN under Ar (red line), CO_2 (blue line), and CO_2 in the presence of 2.65 M H_2O (purple line). Working electrode, glassy carbon; counter electrode, Pt wire; reference electrode, Ag/Ag^+; scan rate, 0.1 V s^{-1}. Potential sweeps were started from the open-circuit potential for all measurements.

is induced by the strong σ-donating and relatively weak π-accepting nature of the phosphine ligand[25]. Such an interaction largely contributes to CO_2 reduction under mild conditions (i.e. at a low overpotential). Thus, the importance of the NHC ligand in enhancing the interaction of the complex with CO_2 was confirmed.

Encouraged by the aforementioned results, we investigated the catalytic activity of **RuC** for visible-light-driven CO_2 reduction. Photocatalytic CO_2 reduction was conducted under visible-light irradiation (420 ≤ λ ≤ 750 nm) in a CO_2-saturated MeCN/H_2O (39:1, v:v) solution containing **RuC** (20 μM) as a catalyst and 1,3-dimethyl-2-phenyl-2,3-dihydro-1*H*-benzo[d]imidazole (BIH, 0.1 M) as a sacrificial electron donor. The evolution of CO was observed, and negligible amounts of H_2 were detected (Table 1, Entry 1). No induction period was

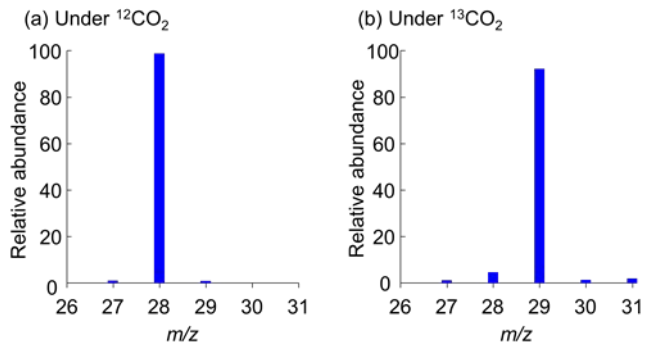

Fig. 4 Mass spectra of CO generated under (a) $^{12}CO_2$ and (b) $^{13}CO_2$ using a MeCN/H_2O (39:1, v:v) solution containing 20 μM RuC and 0.1 M BIH at 20 °C upon irradiation with a Xe lamp (420 ≤ λ ≤ 750 nm) for 3 h.

observed during catalysis, which indicates the instant formation of catalytically active species upon photoirradiation. To verify the role of each component in the photoreaction, we conducted a series of control experiments. No CO was observed when the reaction was performed without **RuC**, without BIH, in the dark, and under Ar (Table 1, entries 3–6); these findings demonstrate that **RuC** is the photocatalyst, BIH functions as the sacrificial electron donor, and CO_2 is the substrate. Isotopic-labelling experiments performed under a $^{13}CO_2$ atmosphere confirmed that the CO obtained originated from CO_2 reduction (Fig. 4). The turnover number of **RuC** for CO production after 3 h of reaction reached 110, which corresponds to a TOF of 36.7 h^{-1}. This TOF value is over two-fold greater than that of **RuP** (16.0 h^{-1}), which is an example of a Ru-based function-integrated catalyst for visible-light-driven CO_2 reduction, under identical conditions (Table 1, Entry 2). More importantly, the TOF of **RuC** is the highest among those of previously reported function-integrated catalysts for visible-light-driven CO_2 reduction (Table S7). These results clearly demonstrate that the introduction of the NHC ligand to the Ru polypyridyl scaffold is an attractive strategy for obtaining an efficient catalyst.

Finally, we propose a possible catalytic mechanism for the photochemical reduction of CO_2 by **RuC**, as shown in Fig. S19. Initially, the photoexcited state of **RuC** is reductively quenched by BIH to form $[Ru^{II}(tpy^-)(cpic)(MeCN)]^+$ (**RuC**$^-$), as evidenced by CV (*vide supra*). The ligand-exchange reaction between MeCN and CO_2 subsequently proceeds to form the CO_2 adduct, $[Ru^{II}(tpy)(cpic)(CO_2^{\bullet-})]^+$ (**RuC**$_{CO_2}^{\bullet-}$). DFT calculations (Fig. S16) revealed that the HOMO of **RuC**$_{CO_2}^{\bullet-}$ is mainly localised on the metal-bound CO_2, thus suggesting that intramolecular electron transfer from the tpy moiety to CO_2 proceeds upon the exchange of the MeCN ligand. The HOMO of **RuC**$_{CO_2}^{\bullet-}$ is also located on the cpic ligand, which indicates that the cpic ligand contributes to the stabilisation of the Ru-C($CO_2^{\bullet-}$) bond of **RuC**$_{CO_2}^{\bullet-}$ via π-back donation. **RuC**$_{CO_2}^{\bullet-}$ undergoes further one-electron reduction, and the subsequent protonation reaction forms the intermediate $[Ru^{II}(tpy^-)(cpic)(CO_2H)]^+$. Further protonation and dehydration of $[Ru^{II}(tpy^-)(cpic)(CO_2H)]^+$ afford the CO-coordinated species, $[Ru^{II}(tpy)(cpic)(CO)]^{2+}$ (**RuC**$_{co}$).[5] Finally, the ligand-exchange reaction of **RuC**$_{co}$ produces CO as a major product and closes the catalytic cycle.

Table 1. Control experiments for photocatalytic CO_2 reduction by **RuC** for 3 h.

Entry	Catalyst (μM)	Electron donor	λ (nm)	gas	Products (TON)	
					CO	H_2
1	**RuC** (20)	BIH	420 ≤ λ ≤ 750	CO_2	110	1
2	**RuP** (20)	BIH	420 ≤ λ ≤ 750	CO_2	55	1
3	-	BIH	420 ≤ λ ≤ 750	CO_2	0	0
4	**RuC** (20)	-	420 ≤ λ ≤ 750	CO_2	0	0
5	**RuC** (20)	BIH	Dark	CO_2	0	0
6	**RuC** (20)	BIH	420 ≤ λ ≤ 750	Ar	0	0

In summary, we have designed and synthesised a novel Ru polypyridyl complex bearing an NHC ligand, **RuC**. The complex was successfully characterised using several experimental techniques. UV-vis absorption spectroscopy and electrochemical measurements clarified the importance of the NHC ligand for enhancing the absorption properties and affinity of the complex to CO_2 molecules. **RuC** effectively promoted the visible-light-driven reduction of CO_2 as a function-integrated catalyst (i.e. without an additional photosensitiser). **RuC** demonstrated excellent catalytic performance. Specifically, the TOF of the complex, 36.7 h^{-1}, was over two-fold greater than that of **RuP** and higher than those of previously reported function-integrated catalysts of the same class. The current study offers a novel design principle for constructing efficient function-integrated catalysts for visible-light-driven CO_2 reduction. Note that the stability of our system should be improved in future (Fig.S12).

This work was supported by Grants-in-Aid for Scientific Research (KAKENHI) (Grant Numbers 17H06444, 19H00903, and 20K21209 (S.M.); Grant Numbers 15H05480, 17K19185, 17H05391, 19H04602, 19H05777, and 20H02754 (M. K.)), and (Grant Number 20K15955 (Y.S.)) from the Japan Society for the Promotion of Science. This work was also supported by JST PRESTO (Grant Number JPMJPR20A4 (M. K.)) and JST CREST (Grant Number JPMJCR20B6 (S. M.)), Japan, Iketani Science and Technology Foundation (M. K.), Izumi Science and Technology Foundation (M. K.), and Mazda Foundation (M. K.). The computations were performed at the Research Center for Computational Science, Okazaki, Japan.

Conflicts of interest

There are no conflicts to declare.

Notes and references

1 K. Li, B. Peng and T. Peng, *ACS Catal*., **2016**, *6*, 7485–7527.
2 G. Sahara and O. Ishitani, *Inorg. Chem*., **2015**, *54*, 5096–5104.
3 E. Boutin, L. Merakeb, B. Ma, B. Boudy, M. Wang, J. Bonin, E. Anxolabéhère-Mallart and M. Robert, *Chem. Soc. Rev*., **2020**, *49*, 5772–5809.
4 R. Cauwenbergh and S. Das, *Green Chem*., **2021**, *23*, 2553–2574.
5 S. K. Lee, M. Kondo, M. Okamura, T. Enomoto, G. Nakamura and S. Masaoka, *J. Am. Chem. Soc*., **2018**, *140*, 16899–16903.
6 J. Hawecker, J.-M. Lehn and R. Ziessel, *J. Chem. Soc. Chem. Commun*., **1983**, 536–538.
7 J. Hawecker, J.-M. Lehn and R. Ziessel, *Helv. Chim. Acta*, **1986**, *69*, 1990–2012.
8 H. Hori, F. P. A. Johnson, K. Koike, O. Ishitani and T. Ibusuki, *J. Photochem. Photobiol. A*, **1996**, *96*, 171–174.
9 A. J. Huckaba, E. A. Sharpe and J. H. Delcamp, *Inorg. Chem*., **2016**, *55*, 682–690.
10 A. Maurin, C.-O. Ng, L. Chen, T.-C. Lau, M. Robert and C.-C. Ko, *Dalton Trans*., **2016**, *45*, 14524–14529.
11 Y. Hameed, P. Berro, B. Gabidullin and D. Richeson, *Chem. Commun*., **2019**, *55*, 11041–11044.
12 J. Bonin, M. Chaussemier, M. Robert and M. Routier, *ChemCatChem*, **2014**, *6*, 3200–3207.
13 H. Rao, J. Bonin and M. Robert, *Chem. Commun*., **2017**, *53*, 2830–2833.
14 S. Sato, T. Morikawa, T. Kajino and O. Ishitani, *Angew. Chem. Int. Ed*., **2013**, *52*, 988–992.
15 R. O. Reithmeier, S. Meister, B. Riegar, A. Siebel, M. Tschurl, U. Heiz and E. Herdtweck, *Dalton Trans*., **2014**, *43*, 13259–13269.
16 R. O. Reithmeier, S. Meister, A. Siebel and B. Rieger, *Dalton Trans*., **2015**, *44*, 6466–6472.
17 K. Garg, Y. Matsubara, M. Z. Ertem, A. Lewandowska-Andralojc, S. Sato, D. J. Szalda, J. T. Muckerman and E. Fujita, *Angew. Chem. Int. Ed*., **2015**, *54*, 14128–14132.
18 A. Genoni, D. N. Chirdon, M. Boniolo, A. Sartorel, S. Bernhard and M. Bonchio, *ACS Catal*., **2017**, *7*, 154–160.
19 S. Sato and T. Morikawa, *ChemPhotoChem*, **2018**, *2*, 207–212.
20 K. Kamada, J. Jung, T. Wakabayashi, K. Sekizawa, S. Sato, T. Morikawa, S. Fukuzumi and S. Saito, *J. Am. Chem. Soc*., **2020**, *142*, 10261–10266.
21 J. Chauvin, F. Lafolet, S. Chardon-Noblat, A. Deronzier, M. Jakonen and M. Haukka, *Chem. - Eur. J*. **2011**, *17*, 4313–4322.
22 C. E. Castillo, J. Armstrong, E. Laurila, L. Oresmaa, M. Haukka, J. Chauvin, S. Chardon-Noblat and A. Deronzier, *ChemCatChem*, **2016**, *8*, 2667–2677.
23 S. Das, R. R. Rodrigues, R. W. Lamb, F. Qu, E. Reinheimer, C. M. Boudreaux, C. E. Webster, J. H. Delcamp and E. T. Papish, *Inorg. Chem*., **2019**, *58*, 8012–8020.
24 G. Nakamura, M. Okamura, M. Yoshida, T. Suzuki, H. D. Takagi, M. Kondo and S. Masaoka, *Inorg. Chem*., **2014**, *53*, 7214–7226.
25 S. K. Lee, M. Kondo, G. Nakamura, M. Okamura and S. Masaoka, *Chem. Commun*., **2018**, *54*, 6915–6918.
26 M. N. Hopkinson, C. Richter, M. Scherdler and F. Glorius, *Nature*, **2014**, *510*, 485–496.
27 S. Gonell, E. A. Assaf, K. D. Duffee, C. K. Schauer and A. J. M. Miller, *J. Am. Chem. Soc.*, **2020**, *142*, 8980-8999.
28 J. Thongpaen, R. Manguin and O. Baslé, *Angew. Chem. Int. Ed.*, **2020**, *59*, 10242-10251.
29 W. A. Herrmann and C. Köcher, *Angew. Chem. Ed. Engl*., **1997**, *36*, 2162–2187.